ANL/PPRNT--89-187

DE90 002997

TIME-DEPENDENT ASPECTS OF ELECTRON DEGRADATION.
IV. SUBEXCITATION ELECTRONS IN NITROGEN AND CARBON DIOXIDE[*]

Mineo Kimura,[†] Mitio Inokuti, Ken-ichi Kowari[‡],
Michael A. Dillon, and Antonio Pagnamenta[§]
Argonne National Laboratory, Argonne, Illinois 60439

Abstract

We discuss here the temporal behavior of subexcitation electrons and the yields of products due to these subexcitation electrons. Our examples concern cases in which resonance scattering of electrons occurs, such as vibrational and rotational excitation in N_2 and negative-ion formation in CO_2. One focus of the present work is a test of the continuous-slowing-down-approximation (CSDA) which we compare to the full solution of the time-dependent Spencer-Fano theory, which has been developed recently.

---

[*] Work supported in part by the U.S. Department of Energy, Office of Health and Environmental Research, under Contract W-31-109-Eng-38, and by Office of Basic Energy Sciences.

[†] Also, Rice University, Houston, Texas 77251.

[‡] Visiting Scientist. Permanent address: 7-37-21 Minamikoiwa, Edogawa-ku, Tokyo, Japan.

[§] Department of Physics, University of Illinois, Chicago, Illinois 60680

I. INTRODUCTION

Electrons whose energies are below the first electronic excitation threshold are termed "subexcitation electrons."[1] These electrons lose their energy mainly through vibrational excitations, rotational excitations, or elastic collisions; thus, the rate of energy loss in these collision processes is much smaller than the rate of energy loss of more energetic electrons that are capable of electronic excitation. In addition, no secondary electrons are generated in the subexcitation region. Hence, the subexcitation electrons allow us to adopt a treatment that is conceptually far simpler than that for more energetic electrons.

The role of the subexcitation electrons becomes especially conspicuous when the irradiated medium contains small amounts of impurity substances whose excitation or ionization energies are below the first threshold of electronic excitation of the major constituent. Impurity molecules can then be excited or ionized by the subexcitation electrons and can trigger observable consequences. For instance, the addition of impurities of different rare-gases in helium gives rise to different amounts of increase in the total ionization, as discussed by Platzman.[1]

Subexcitation electrons are also responsible for vibrational and rotational excitation in molecules and negative-ion formation followed by dissociative electron attachment to molecules. It has been also recognized for some time that various astrophysical phenomena are attributable to the subexcitation electrons, or slow electrons in general.[2] Because of the small mean energy loss per collision and of the production of no secondary electrons in the subexcitation domain, the continuous-slowing-down approximation (CSDA) is believed to be a good approximation to describe the electron degradation. Indeed, Dillon, Inokuti, and Kimura in Paper I of the present series[3] used the

CSDA, and successfully interpreted the experimental finding of the time-dependence of the production of excited N_2 by subexcitation electrons in rare-gas mixtures. However, it is desirable to conduct a thorough study for testing the validity of the CSDA in both time-independent and time-dependent cases.

Interesting questions are how resonance and negative-ion formation (for which the cross sections are sharply dependent on energy) affect the validity of the CSDA and how the yields of these processes evolve as a function of time. These questions are relevant to primary events in radiation chemistry and biology.

The present report has two aims: (i) to discuss results of our systematic study for testing the CSDA in time-dependent and time-independent cases; and (ii) to illustrate time-dependent aspects of degradation spectra and of yields of various species in two selected examples, the N_2 molecule, which has the well-known, strong shape resonance at about 2.5 eV; and the CO_2 molecule, for which negative-ion formation due to dissociative attachment is known. Our work was stimulated by recent theoretical studies on the moderation of subexcitation electrons,[4,5] that treat stationary cases within the CSDA.

II. THEORY

A full account of the time-dependent treatment of electron degradation, referred to as the time-dependent Spencer-Fano (TDSF) theory, has been presented elsewhere (Paper II).[6] Therefore, a brief outline of the theory will suffice to make the present note self-consistent. The TDSF equation for the incremental electron degradation spectrum $z(T_0, T; t)$ is written as

$$\frac{1}{v_T} \frac{\partial z(T_o,T;\ t)}{\partial t} = nK_T z(T_o,T;\ t) + \delta(T_o - T)\ \delta(t), \qquad (1)$$

where v_T is the speed of an electron of energy T, n is the number density of molecules in the medium, and T_0 is the initial kinetic energy of the electron at time t = 0. The cumulative degradation spectrum $Z(T_0, T; t)$ is defined by

$$Z = \int_0^t z(T_0, T; \lambda)d\lambda \qquad (2)$$

and

$$Z \to y(T_0, T) \qquad t \to \infty, \qquad (3)$$

where $y(T_0, T)$ is the steady-state degradation spectrum of Spencer and Fano.[6] The symbol K_T represents the cross-section operator that is fully discussed in Paper II.[6] In summary, $nK_Tz(T_0, T; t)$ represents the net increase in the electron degradation spectrum due to all collisions with molecules. Equation (1) represents the overall balance of the number of electrons at time t, with energy T, if the initial electron had energy T_0.

Within the CSDA, Eq. (1) can be simplified to

$$\frac{\partial[s(T)\ z(T_0, T; t)]}{\partial t} = - \frac{\partial[s(T)\ z(T_0, T; t)]}{\partial x} + v_T s(T)\delta(T - T_0)\delta(t), \qquad (4)$$

where s(T) is the stopping cross section for electrons at energy T and is defined by

$$s(T) = \sum_j E_j \sigma_j(T), \qquad (5)$$

$\sigma_j(T)$ is the cross section for a collision with energy loss of E_j, and

$$x = \int_T^{T_0} \frac{d\lambda}{nv_\lambda s(\lambda)} \quad . \qquad (6)$$

The variable x has the dimension of time. It represents the time in which the energy of an electron decreases from T_0 to T within the CSDA and is termed "the CSD time." Equation (4) can be solved analytically, and the solution has the form

$$z(T,\ t) = \frac{s[g(x-t)]}{s(T)}\, z_0[g(x-t)]\ , \tag{7}$$

where $g(x) = T$ is the inverse of Eq. (6), and z_0 is the initial incremental degradation spectrum.

In specific applications, discussed in the next section, both the exact solution of the TDSF equation (1) and its CSDA version equation (7) are numerically evaluated for a determination of the time-dependent electron degradation $Z(T_0,\ T;\ t)$.

III. EXAMPLES

In the present study we choose N_2 and CO_2, i.e., molecules that show sharp structures in electron-collision cross sections characteristic of resonances. In N_2, there is a strong resonance at 2.5 eV, which causes structures in the momentum-transfer cross section, in the rotational-excitation cross section, and especially in the vibrational-excitation cross section. In CO_2, there is a resonance at 4.2 eV, which leads to the dissociative attachment yielding O^- and to related structures in the cross sections for other processes.

The strong energy dependence of the cross sections implies that the history of an individual electron is highly stochastic, i.e., it strongly depends upon which precise energy it may take during the slowing-down process. However, in the CSDA one visualizes the behavior of a mean electron, representative of many electrons having more or less the same energy. This basic idea of the CSDA is certainly appropriate for the description of the subexcitation electrons in many contexts (as exemplified in Paper I), but is most questionable in the examples we chose in the present work.

Some representative electron scattering cross sections are displayed in Figs. 1 and 2. All cross section data used in the present study are found in Ref. 7 for N_2, and in Refs. 8-10 for CO_2. The first electronic excitation thresholds are 6.2 eV for the N_2 $A^3\Sigma_u^+$ state, and 5.4 eV for the CO_2 $A^3\Pi$ state. Hence, the initial energies of subexcitation electrons in the present study should be below these threshold values. The gas pressure was fixed to one atmosphere for both cases in all calculations. Furthermore, all the molecules are assumed to be in their vibrationally, as well as rotationally, ground state. This assumption corresponds to a gas at zero-degree temperature. A treatment of electron degradation in higher-temperature gases will be deferred to another occasion.

IV. RESULTS

N_2

As seen in Fig. 1, a strong shape resonance due to temporary trapping of an incident electron has a very large effect on all cross sections for N_2 at energies between 1.5 eV and 3.5 eV. This effect is strongest in the vibrational excitation cross sections. In fact, the vibrational excitation cross sections for $v = 0 \rightarrow 1$ and $v = 0 \rightarrow 2$ transitions are very small except near the resonance within the energy region considered. Oscillatory structure is out of phase for $v = 0 \rightarrow 1$ and $v = 0 \rightarrow 2$ transitions.

Rotational-excitation cross sections again show sharp peaks in the resonance region. However, the background magnitude (due to non-resonant scattering) is much larger than that for the vibrational excitation. The rotational excitation cross section sharply increases with energy near the threshold, and then gradually decreases with energy above 0.1 eV. This behavior may be attributed to an interplay of the quadrupole and polarization potentials for electron-N_2 interactions, which is quite in contrast from the case of e - H_2 case, where the cross sections increase monotonically from the threshold.

Shown in Fig. 3 is the CSD time, or moderation time, versus energy for N_2 at one atmosphere. For a fixed gas pressure, there is one-to-one correspondence between the CSD time and energy through Eq. (6). Similar results have been presented by Stephens and Robicheaux[5] for a variety of diatomic molecules, which possess resonances. Several points are worth noting in N_2.

(i) The sharp resonance around 2.5 eV, which causes peaks in the stopping cross section, obviously plays a decisive role in determining the CSD time. As a result, the CSD time at 4 eV is almost identical to that at 1.5 eV, as seen in the flatness of the curve in the middle of Fig. 3.

(ii) Below the rotational excitation threshold, the elastic collision is the sole source of electron degradation. The mean energy loss per elastic collision is exceedingly small because of the factor 2m/M in the stopping cross section (where m is an electron mass and M is a nuclear mass).

(iii) Generally, it is convenient to classify the subexcitation domain into the following regions:

(a) the region where vibrational energy transfer dominates,

(b) the region below the vibrational excitation threshold, where rotational excitation and elastic collisions dominate, and

(c) the region where a specific resonance is observed and therefore the CSD time strongly depends on energy.

In reality these regions overlap each other, and hence the classification is schematic and tentative. Nevertheless, it is helpful for the following discussion of the electron slowing-down process and of the time-dependence of each yield.

Figure 4 illustrate some representative yields as a function of the CSD time. The yields here represent accumulation of each yield as time passes.

The vibrational excitation process is almost complete at the early stage of the slowing-down process, as seen in the drastic increase of the yield at $t < 0.2 \times 10^{-8}$ sec. By contrast, rotational excitation is a rather slow process and its yield receives appreciable contributions from all intervals of the slowing-down time. This is clear from the cross sections shown in Fig. 1. Upon degradation through the resonance region where the vibrational excitation dominates, the yield of vibrational excitation increases almost like a step function. In contrast, the rotational excitation cross section shows characteristic "arms" on both the lower and higher energy sides of the resonance region. This causes the rapid increase in the yield at an early time and the more gradual increase in the yield at a later time, i.e., after the vibrational excitation is completed. It should be noted that in a region where vibrational excitation abruptly increases, the rate of increase in the rotational excitation yield becomes correspondingly slower, although this is not seen clearly in Fig. 4. This is so because all energy losses of electrons are virtually exhausted by the vibrational excitation processes in this region.

It may be appropriate to assess the validity of the CSDA here. Our systematic study clearly shows that the CSDA result is in excellent accord with the solution of the TDSF equation within a few percent except for the

Lewis effect (viz., the sharp structure slightly below the source energy, which arises from the small number of collisions involved). Yet the TDSF solution is more sensitive to the shape of cross sections used and displays much more of finer structures in the degradation spectrum. A more detailed discussion concerning the comparison of the TDSF with the CSDA will be presented elsewhere.[11] Overall, the CSDA turns out to give remarkably good results even in the presence of resonances.

CO_2

Major cross sections are displayed in Fig. 2. An important process is the negative-ion formation through electron attachment to the CO_2 molecule. This is dissociative electron attachment (DEA): $e + CO_2 \rightarrow CO + O^-$, which has been studied in several experiments.[8] The dissociative electron attachment cross section has two separate peaks with magnitudes of 1×10^{-19} cm^2 at 4 eV and 4×10^{-19} cm^2 at 8 eV. However, the electronic-excitation threshold is 5.4 eV, and thus the 8-eV peak cannot compete effectively with electronic excitation. Therefore, it contributes little to the negative-ion yield.

The peak at 4 eV is well recognized to have a strong influence on vibrational excitation as well as elastic-collision cross sections, as is apparent from Fig. 2. The CO_2 molecule has three fundamental modes of vibration: namely, the (100), (010), and (001) modes with respective thresholds[9] at 0.172 eV, 0.0827 eV, and 0.283 eV. Recent theoretical and experimental studies[9,10] have shown the enhancement of the vibrational excitation cross section near the threshold in all three channels resulting from virtual-state effects. The cross-section magnitude decreases monotonically in the higher-energy side except for resonance structure. It should be noted that the rotational constant B for the CO_2 is very small;

therefore, its "elastic-collision cross section" reported in experiments includes effects of rotational transitions as well. In this sense, the term "elastic" in the present context really means vibrationally elastic.

The CSD time in CO_2 again at one atmosphere versus energy is shown in Fig. 5. It is instructive to compare CO_2 to N_2 in several respects:

(i) For CO_2 (which has no strong resonance), the CSD time is longer, owing to a smaller mean energy loss per collision.

(ii) The effect of negative-ion formation to the degradation spectrum is small, only causing a shoulder in the CSD time at 4 eV. Given the small cross section for the DEA, this is certainly expected.

(iii) Below the lowest vibrational excitation threshold, the electron degradation is caused by elastic collisions only. As discussed in the N_2 case, the rate of energy loss in this region is small.

(iv) The general remark concerning the classification of the slowing-down regions made in (iii) in the N_2 case also holds here.

The yields for vibrational excitations and negative-ion formation are plotted as a function of the CSD time for the CO_2 in Fig. 6. The cross section for the DEA has a sharp pronounced peak at 4 eV as seen in Fig. 2. Therefore, the negative-ion formation occurs only at early stage of the degradation. Next, the sharp increase in the vibrational excitation dominates. Finally, elastic collisions become the sole contributor to the energy loss when electron energies are lower than (010) vibrational excitation threshold 0.08 eV. The magnitude of yields is related to a mean of each cross section. Clearly, the order of the yields for the three vibrational excitations seen in Fig. 6 agrees with the order of the corresponding cross sections in Fig. 2.

The yields for N_2 and CO_2 cases obtained at various terminal energies are listed in Table I.

CONCLUSIONS

The present study shows that the CSDA gives reasonably accurate results in the subexcitation region and yet it is economical in practical computation. On the basis of the size of each quanta transferred to vibrational or rotational excitation, we find it appropriate to classify the subexcitation domain into two regions, namely, (i) the region where vibrational excitation dominates, and (ii) the region where rotational excitation and elastic collision dominate. Undoubtedly, the presence of a resonance causes a major influence on the energy-loss process. However, the influence sensitively depends upon its magnitude and location, and hence consequences to the yield and the slowing-down time are different for different molecules.

For gaseous mixtures, it is interesting to study time-dependent aspects of the yields when one or two cross sections for inelastic molecular collisions are exceedingly large in the subexcitation domain. For example, it is well known that certain types of charge transfer and reactions in ion-molecule collisions are extremely fast. This topic may well be important in the considerations of early events in radiation chemistry and biology.

ACKNOWLEDGEMENT

This work is supported in part by the U.S. Department of Energy, Office of Health and Environmental Research, under Contract W-31-109-Eng-38 and in part by the Division of Chemical Sciences, Office of Basic Energy Sciences. We also acknowledge the award of the CRAY time necessary for our computation.

Table 1. Yields of various species for N_2 and CO_2.

T_0: initial energy; T_{end}: terminal energy

Product	N_2 yields (T_0 = 6.2 eV; T_{end} = 0.02 ev)
vibrational excitation	
(0 → 1)	13.9
rotational excitation	
(0 → 2)	377.8
(0 → 4)	168.5
(0 → 6)	17.2
(0 → 8)	11.8

Product	CO_2 yields (T_0 = 5.4 eV; T_{end} = 0.05 eV)
vibrational excitation	
(010)	4.0
(100)	5.8
(001)	12.4
O^- formation	0.011

References

1. R. L. Platzman, Radiat. Res. 2, 1 (1955).
2. T. E. Cravens, G. A. Victor, and A. Dalgarno, Planet. Space. Sci. 23, 1059 (1975).
3. M. A. Dillon, M. Inokuti, and M. Kimura, Rad. Phys. Chem. 32, 43 (1988).
4. D. A. Douthat, Astrophys. J. 314, 419 (1987).
5. J. A. Stephens and F. Robicheaux, Radiat. Res. 110, 19 (1987).
6. M. Inokuti, M. Kimura, and M. A. Dillon, Phys. Rev. A XX, XXX (1988).
7. Y. Itikawa, M. Hayashi, A. Ichimura, K. Oda, K. Sakimoto, K. Takayanagi, M. Nakamura, H. Nishimura, and T. Takayanagi, J. Phys. Chem. Ref. Data 15, 985 (1986).
8. Y. Itikawa and M. Shimizu, Bull. Inst. Space and Aeronaut. Sci., Univ. Tokyo 7, 64 (1971).
9. Vibrational-excitation cross sections were calculated using a quantum mechanical close-coupling method by Kimura and Lane and published in Phys. Rev. A XX, XXX (1988).
10. Recent experimental measurement by K.-H. Koem, W. Sohn, N. Habel, J. Jung, and H. Ehrhardt, J. Phys. B 18, 4455 (1985), supports theoretical results by Kimura and Lane in Ref. 9b.
11. K. Kowari, M. Kimura, and M. Inokuti, to be published.

Figure Captions

Fig. 1. Momentum transfer, rotational excitation ($0 \rightarrow 2$) and vibrational excitation ($0 \rightarrow 1$) cross sections for e + N_2 collisions.

Fig. 2. Momentum transfer and vibrational excitation cross sections for e + CO_2 collisions.

Fig. 3. The CSD-time versus energy for N_2.

Fig. 4. Various yields versus time for N_2. Note the CSD-time in bottom scale and the corresponding energy in top scale.

Fig. 5. The CSD-time versus energy for CO_2. Note small structure at $E \approx 4$ eV due to the negative-ion formation.

Fig. 6. Various yields versus time for CO_2. Note the CSD-time in bottom scale and the corresponding energy in top scale.

Figure 1

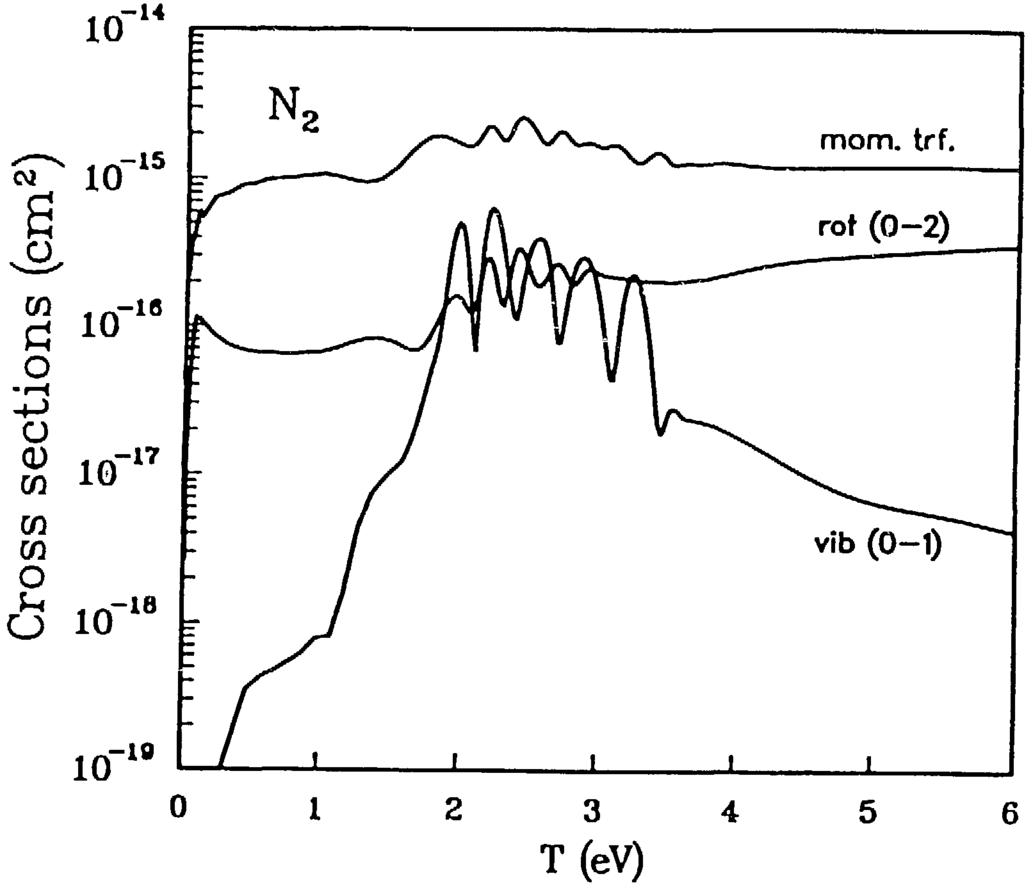

10^{-14}
10^{-15}
10^{-16}
10^{-17}
10^{-18}
10^{-19}
Cross sections (cm^2)
N_2
mom. trf.
rot (0–2)
vib (0–1)
0
1
2
3
4
5
6
T (eV)

Figure 2

T2-CO2SIG

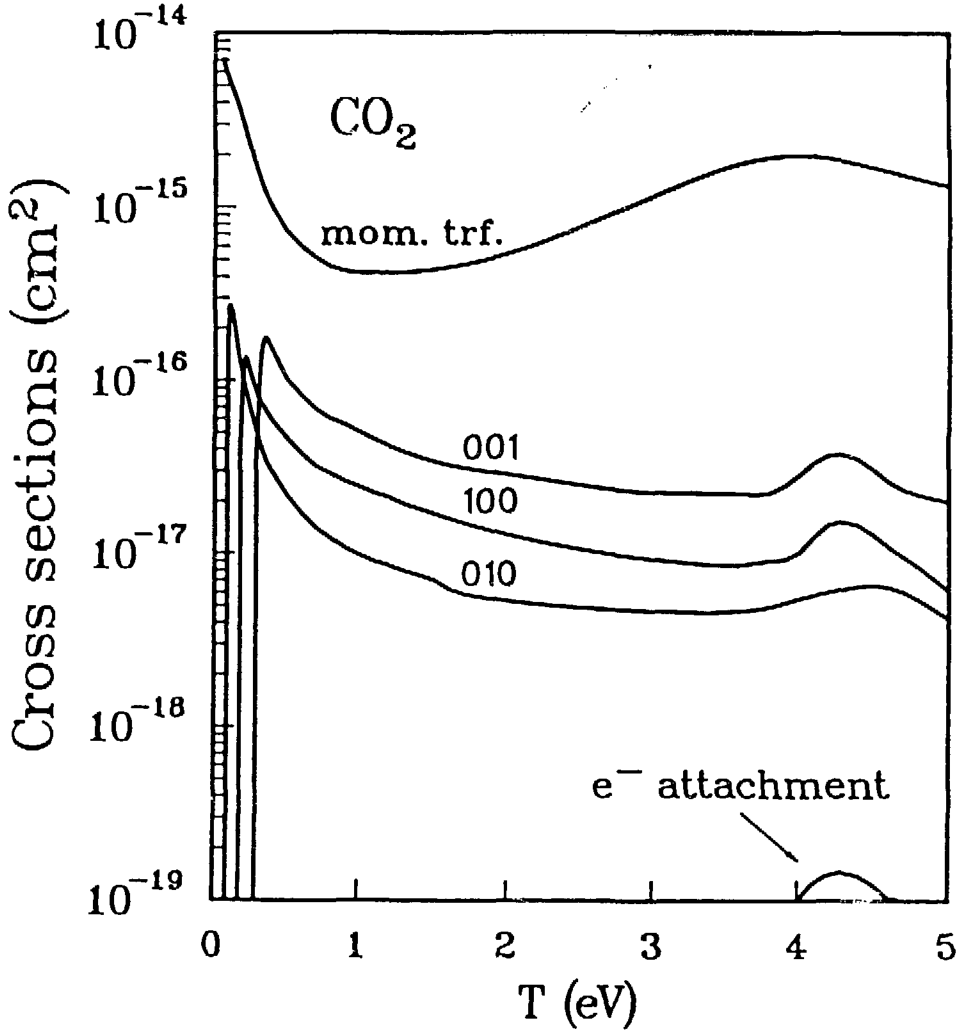

Figure 3

T3-N2TIME

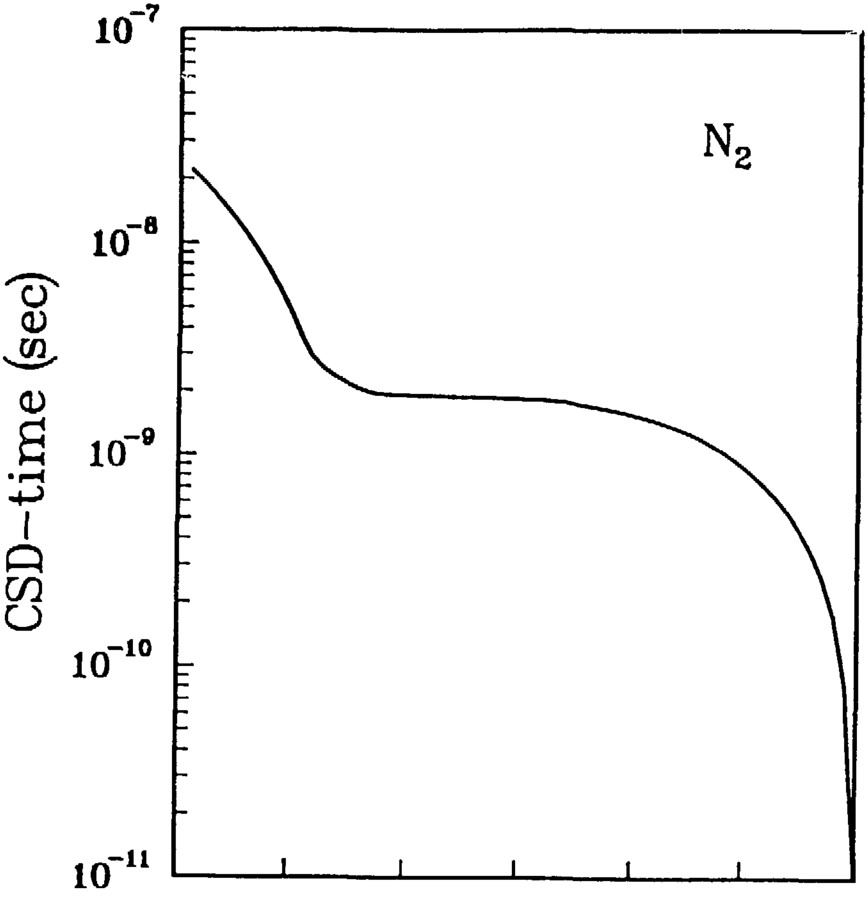

Figure 4

T4N2YIET

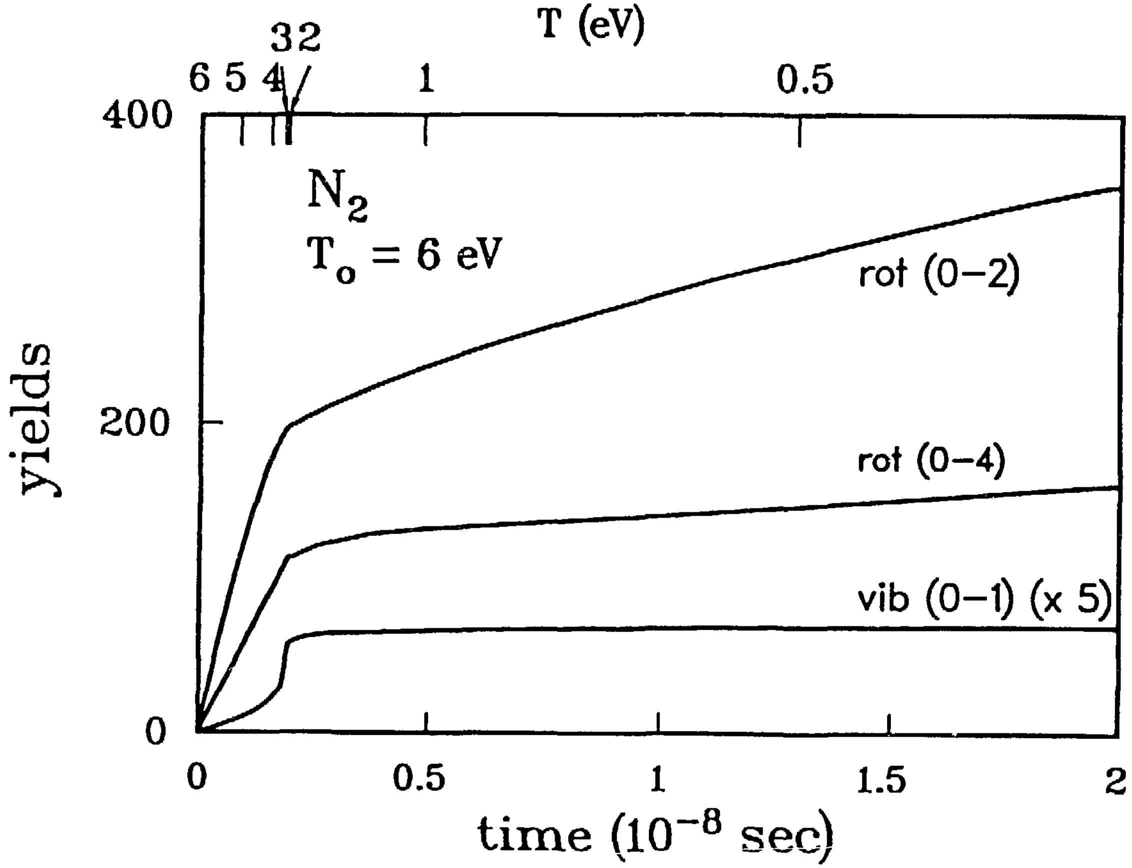

Figure 5

TSCO2TIM

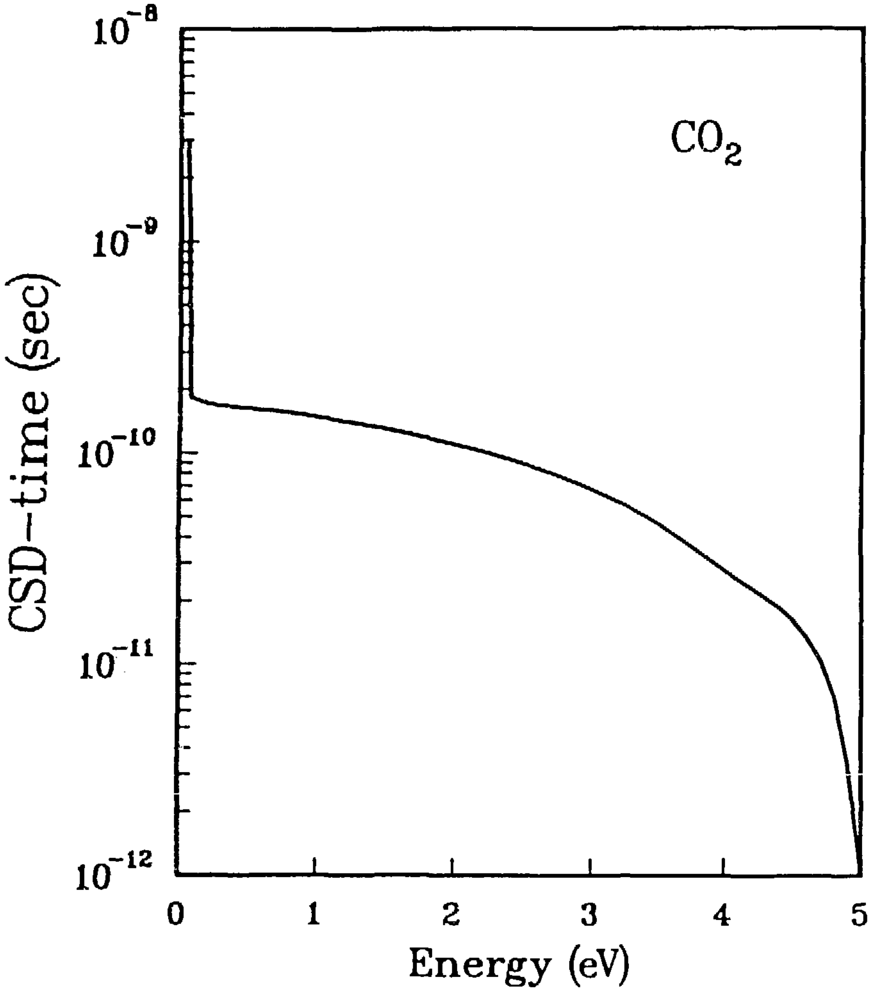

Figure 6

T6-CO2YT